

## Experimental electrical resistivity and thermopower of molten germanium interpreted with muffin-tin potential calculations

This article has been downloaded from IOPscience. Please scroll down to see the full text article.

1999 J. Phys.: Condens. Matter 11 671

(<http://iopscience.iop.org/0953-8984/11/3/007>)

View [the table of contents for this issue](#), or go to the [journal homepage](#) for more

Download details:

IP Address: 171.66.16.210

The article was downloaded on 14/05/2010 at 18:35

Please note that [terms and conditions apply](#).

## Experimental electrical resistivity and thermopower of molten germanium interpreted with muffin-tin potential calculations

A Makradi†, J G Gasser†§, J Hugel‡, A Yazici† and M Bestandji†

† Laboratoire de Physique des Liquides et des Interfaces, 1 Boulevard Arago,  
57 078 Metz Cédex 03, France

‡ Laboratoire de Spectrométrie Optique de la Matière, 1 Boulevard Arago,  
57 078 Metz Cédex 03, France

Received 26 June 1998, in final form 16 October 1998

**Abstract.** We present our new accurate measurements on the electrical resistivity and thermopower of liquid germanium as a function of temperature. To interpret our data we used *ab initio* calculations of the electrical resistivity  $\rho(E)$  and of the thermoelectric power  $Q(E)$  of liquid germanium as a function of energy. The calculations have been performed within a self-consistent method in which the conduction band bottom has been matched with the muffin tin zero. Various potentials have been used especially the potential based on the Hartree–Fock formalism and the potential derived from the density functional theory which take into account the exchange and correlation effects. As result the new prescriptions improve significantly the resistivity and the thermopower with respect to the methods commonly used.

### Introduction

With the development of new theoretical models and computing techniques, several authors focused their attention on the interpretation of the unusual atomic and electronic experimental properties of liquid polyvalent metals like germanium. The radial distribution function of this liquid ‘metal’ does not display the usual minimum in the region between the first and the second main peaks; a flat maximum is located in this region [1]. The corresponding static structure factor  $a(q)$  shows an important deviation from a hard-sphere-like structure factor, with a small shoulder on the high side of the first peak at about  $q = 2k_F$ . For germanium the number of nearest neighbours is estimated to be 6.8 by Bellissent *et al* [2], compared to 11 for liquid aluminium, which suggests that some remanence of the crystalline tetrahedral network occur. The electronic density of states has been obtained by the photoemission experiments of Indelkofer *et al* [3] which show a clear separation of the s and p states in the middle of the conduction band of liquid germanium and a minimum at the Fermi energy. This DOS configuration is related to the low value of the first nearest neighbour co-ordination (lower than seven), which yields a reduction of the overlap between orbitals centred on the neighbouring sites. This interplay of the atomic order and of the electronic structure has been interpreted by Jank and Hafner [4] using pseudopotential perturbation theory. The latter authors showed that the screening of the ions by the conduction electrons leads to the Friedel oscillations in the interatomic potential. The ions are located in Friedel’s minimum at a distance of about

§ Corresponding author: Professor Jean Georges Gasser, Laboratoire de Physique des Liquides et des Interfaces (LPLI), 1 Boulevard Dominique François Arago, 57078 Metz Cédex 03, France. E-mail address: gasser@lpli.sciences.univ-metz.fr.

$\lambda_F = 2\pi/2k_F$ . Jank and Hafner [4] showed further that if the first nearest neighbour's position is superimposed on the repulsive hump of the interatomic potential, it causes a shoulder in  $a(q)$ .

The electronic properties of liquid metals are based on the scattering of nearly free electrons by potentials. Two different approaches have been followed.

- The first one is based on what Ziman [5] called the 'method of the neutral pseudoatoms'. It consists of starting with the muffin-tin potential of an atom and correcting it by taking into account the exchange through a Slater [6] (or Kohn–Sham [7]) formula. This method has first been used for liquid metals by Dreirach [8] and for liquid alloys by Dreirach *et al* [9], Hirata *et al* [10] and most of the other authors.

- The second is another interesting approach proposed by Ratti and Jain [11, 12]. It consists of constructing the muffin-tin potential of an ion and adding an electronic contribution determined more accurately from the dielectric screening function that includes exchange and correlation. This dielectric screening function was well described and very accurately calculated in pseudopotential calculations of liquid metal transport properties. This description, though more satisfactory from a physical point of view, did not give good results and was no longer used.

The construction of muffin tin potentials needs the knowledge of the interatomic distance to make the superposition of the atomic (or ionic) potentials. Here again two methods have been proposed.

- The first one was that of Dreirach [8] called the quasicrystalline approximation (Q.C.A.) derived from crystalline solids. It takes as input the nearest neighbour distance and the coordination number.

- The second method is that which has been refined by Mukhopadhyay *et al* [13] who constructed the superposition potential by weighting the superposition of the neighbour potentials by the experimental pair correlation function. Waseda [14] and co-workers measured systematically (in the seventies) the structure factors of most metals and calculated the resistivity and thermopower within this method.

The muffin-tin radius is sometimes considered as an adjustable parameter but can be also be reasonably fixed at half the distance of the first peak (maximum) position in the experimental pair correlation function. In our calculations we used this determination of the muffin-tin radius without any fitting. The electronic transport properties depend severely on the pair correlation function used and on the accuracy of its experimental determination.

A very important point is the position of the Fermi energy with respect to the scattering muffin-tin potential. The location depends on the position of the conduction band bottom relative to the muffin-tin zero and on the shape of the density of states.

- Dreirach [8] assumed a free electron band whose bottom is shifted by  $E_B$  from the muffin-tin zero. The  $E_B$  value is calculated following an expression due to Ziman [15].

- On the other hand, Esposito *et al* [16] took  $E_B = 0$  but calculated the density of states with Lloyd's [17] expression.

- We propose an alternative way for the determination of the Fermi energy that will be compared to the above methods mentioned before.

A further matter of discussion is the description of exchange and correlation. It has been included in Ratti's approach through the dielectric screening function. In the muffin-tin approach, the exchange is included in the  $\alpha$  exchange potential coefficient, which was usually taken as 1 (Slater approach) or 2/3 (Kohn–Sham approach). We proposed a better description of the exchange and correlation effects by using either the derivation due to Robinson *et al* [18] or the LDA [19] approach with or without a GGA correction [20, 21].

We present a detailed calculation of the resistivity and of the thermoelectric power for liquid germanium in terms of the  $t$ -matrix approach. The purpose of this paper is first to review the different approaches used to determine the electronic transport properties of liquid metals:

- construction of the atomic or ionic potential;
- methods of superposition of the atomic potentials to construct a disordered condensed matter potential and
- determination of the Fermi energy.

The inconsistencies of the different calculations are discussed. Some results near the experimental values have been obtained earlier (probably fortuitously). In this paper we determine the resistivity and thermopower curve versus energy in order to analyse the influence of the position of the Fermi energy. We introduce the exchange and correlation contribution either with Robinson's expression or with the recent density functional theory using the local density approximation.

The different muffin-tin potentials used in this work are described in section 1. The position of the Fermi energy is discussed in section 2. The Ziman nearly free electron model for electronic transport in liquid metals [22] is presented in section 3. The calculated electronic transport properties of liquid germanium are discussed and compared to our experimental data in section 4.

## 1. Muffin-tin potentials

The phase-shifts entering the expression of the electronic properties are calculated from a muffin-tin potential. The various potentials used in this work divide into three types: potentials derived from the Hartree–Fock theory, potentials obtained within the density functional theory together with different exchange–correlation approximations and ionic potentials.

### 1.1. Hartree–Fock formalism

In the framework of the Hartree–Fock (HF) theory, the atomic one particle potential is given by:

$$v_a(r) = -\frac{z}{r} + \int \frac{\rho(r-r')}{|r-r'|} dr' + v_{ex}(r) \quad (1)$$

where  $z$  is the atomic number. The first and second terms are the potentials due respectively to the Coulomb interaction with the nuclear charge and with the other electrons. The last term is the exchange and correlation potential. The exchange contribution has been approximated by Slater [6] who introduced a weighted average over occupied states.

$$v_{ex}(r) = -3 \left[ \left( \frac{3}{8\pi} \right) \rho(r) \right]^{1/3} \quad (2)$$

where  $\rho(r)$  is the local density of the system in question. To improve the influence of the electron correlation on the pair interactions, we propose to use the expression which has been established by Robinson *et al* [18]. It consists of replacing the Coulomb interaction  $1/|r-r'|$  in the original Slater treatment of the exchange by  $(1/|r-r'|) \exp(-k_s|r-r'|)$ , where  $k_s = (4k_F/\pi)^{1/2}$  is the screening factor and  $k_F$  is the Fermi momentum. The correlation correction leads to the averaged screened exchange potential, which is now expressed as:

$$v_{av.ex.scr.}(r) = - \left( \left( \frac{3}{8\pi} \rho(r) \right)^{1/3} \frac{4}{\pi} \int_0^1 dx \left( 1 - \frac{3}{2}x + \frac{1}{2}x^3 \right) (2k_F x)^2 V(2k_F x) \right) \quad (3)$$

where

$$V(q) = \frac{v_c(q)}{\varepsilon(q)}. \quad (4)$$

The expression  $v_c(q) = 4\pi/q^2$  is the Fourier transform of the Coulomb interaction and  $\varepsilon(q)$  is the electrical dielectric screening function.

### 1.2. Ionic potential

The derivation of Mattheiss describes the dense matter as an assembly of neutral atoms. In metals, it is common to consider that the assembly of ions is immersed in a nearly free electron gas. The pseudopotential theory describes the matter by considering two contributions: an ionic potential (also called bare potential) and an electronic potential. The counterpart in the momentum space is a form factor including the bare ion contribution and the electron contribution through the dielectric screening function. The same ideas have been adopted by Ratti [11, 12] who assumes that the potential seen by a conduction electron is the sum of the ion contribution augmented by its own share of screening cloud. The screened ionic potential is given by:

$$v_s(r) = v_i(r) + v_e(r) \quad (5)$$

where  $v_i(r)$  is the self-consistent *ionic* potential given by Herman and Skillman [23] and Slater [24], which is calculated from equations (1) and (2).  $v_e(r)$  is the screening potential whose Fourier transform  $v_e(q)$  is given by:

$$v_e(q) = \frac{4\pi}{\Omega_0} \left( 1 - \frac{1}{\varepsilon(q)} \right) \quad (6)$$

where  $\varepsilon(q)$  is the well known dielectric screening function including exchange and correlation.

### 1.3. Density functional theory

On the other hand, the density functional method provides a framework for calculation of ground state atomic one-particle potentials. While density functional theory (DFT) [24] is exact in principle, a practical implementation of the method requires the approximation of the exchange–correlation potential. The simplest and most widely approximation used for the exchange–correlation potential is the local-density approximation (LDA) [19], which is valid only for slowly varying densities. The LDA has been improved with the development of the generalized gradient approximation (GGA) [20, 21] in which the exchange–correlation functional incorporates density gradient terms.

For constructing the liquid single site potential, one has to take care of the specific neighbouring arrangement. The construction procedure is the one given by Mattheiss [25] for solids which has been adapted to (disordered) liquid metals by Mukhopadhyay [13]. The atomic environment is introduced by the experimental pair correlation function  $g(r)$  measured by Bellissent-Funel and Bellissent [26]. The liquid single site charge density  $\rho(r)$  and the total coulombic potential  $V_c(r)$  are obtained as follows:

$$\rho(r) = \rho_a(r) + \frac{2\pi}{\Omega_0 r} \int_{R \rightarrow 0}^{\infty} R g(R) dR \int_{R-r}^{R+r} \rho_a(t) dt \quad (7)$$

$$V_c(r) = v_a^c(r) + \frac{2\pi}{\Omega_0 r} \int_{R \rightarrow 0}^{\infty} R g(R) dR \int_{R-r}^{R+r} v_a^c(t) dt \quad (8)$$

where  $\rho_a(r)$  refers to the neutral atom charge density distribution,  $v_a^c(r)$  is the atomic Coulomb potential and  $R$  is the distance of the atom's position from the origin. In the case of the ionic

potential (Ratti's approach) the ionic single site charge density (7) and the total Coulomb ionic potential (8) are obtained by replacing respectively in equations (7) and (8) the neutral atom charge density  $\rho_a(r)$  by the ionic distribution  $\rho_i(r)$  and the atomic Coulomb potential  $v_a^c(r)$  by the ionic one  $v_i^c(r)$ . The muffin-tin potential is written as:

$$V_{MT} = \begin{cases} V_c(r) + V_{ex}(r) & r \leq r_{MT} \\ \varepsilon_{MTZ} & r > r_{MT} \end{cases} \quad (9)$$

where  $V_{ex}(r)$  is the total exchange–correlation potential and  $\varepsilon_{MTZ}$  (the muffin-tin zero) corresponds to the average potential in the interstitial region and is calculated by taking the mean value of potential between the muffin-tin and the Wigner–Seitz spheres:

$$\varepsilon_{MTZ} = \frac{3}{(r_{WS})^3 - (r_{MT})^3} \int_{r_{MT}}^{r_{WS}} r^2 (V_c(r) + V_{ex}(r)) dr. \quad (10)$$

The muffin-tin radius  $r_{MT}$  is taken to be half of the distance between the origin and the first peak in  $g(r)$ . The Wigner–Seitz radius

$$r_{WS} = \left( \frac{3\Omega_0}{4\pi} \right)^{1/3} \quad (11)$$

is expressed as a function of the atomic volume  $\Omega_0$ .

## 2. Fermi energy determination

Two approaches are widely used for the determination of the Fermi energy.

### 2.1. The method of Dreirach *et al*

The earliest one is that given by Dreirach [8] in which the Fermi energy  $E_F$  is written as

$$E_F = E_B + \frac{\hbar^2 k_F^2}{2m^*} \quad (12)$$

where  $E_B$  is the bottom of the band and  $k_F$  is the free electron Fermi wavenumber.  $E_B$  is a structure independent quantity that can be related to the s-phase shift of the muffin-tin potential [15]. The parameter  $m^*$  is an effective mass determined from the band structure in the crystalline state. The energy  $E$  is counted from the muffin-tin zero energy (figure 1) and not from the origin of the free electron density of state.

### 2.2. The method of Esposito *et al*

The second derivation was presented by Esposito *et al* [16] who proposed a consistent method to determine  $E_F$  without any value of  $E_B$  and  $m^*$ . They introduced the number of conduction electrons per atom  $N_C$  (effective valence) which is different from the valence  $Z$ . The Fermi energy  $E_F$  is obtained by filling the density of state curve by  $Z$  electrons. The Fermi wave vector  $k_F$  is obtained from  $E_F$  by:

$$k_F = \frac{(2mE_F)^{1/2}}{\hbar}. \quad (13)$$

The effective valence  $N_C$  is obtained from  $k_F$  by:

$$N_C = \frac{k_F^3 \Omega_0}{3\pi^2}. \quad (14)$$

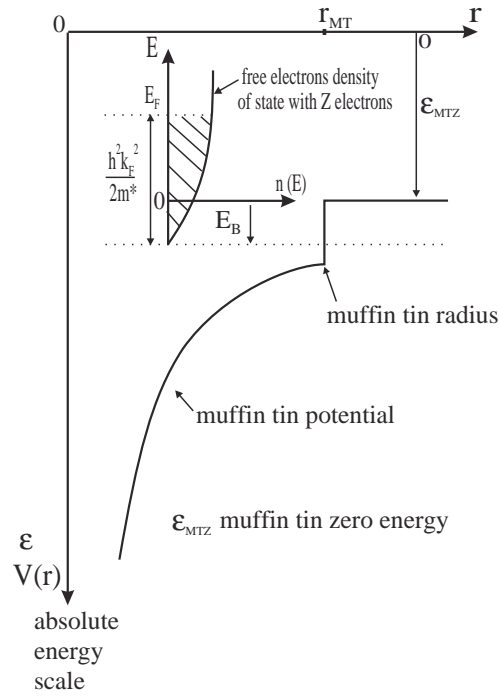


**Figure 1.** Determination of the Fermi energy following the method of Dreirach [8].

The interpretation of this prescription is based on Lloyd's [17] expression for the total integrated density of states per atom appropriate to a system of non-overlapping muffin-tin potentials.

$$N(E) = N_0(E) + \frac{2}{\pi} \sum_l (2l+1) \eta_l(E) + N_m(E). \quad (15)$$

$N_0(E)$  is the free-electron *integrated* density of states proportional to  $(E)^{3/2}$ ,  $\eta_l(E)$  the energy dependent phase shift of the single-site scattering and  $N_m(E)$  the effects of multiple scattering. In order to obtain the Fermi energy together with other free-electron parameters, consistent with the Faber–Ziman formula [27], only single-site scattering has to be taken into account. According to Lloyd [17], this implies that  $E_F$  is to be determined using the total number of valence electrons per atom:

$$Z = N(E_F) \approx N_0(E_F) + \frac{2}{\pi} \sum_l (2l+1) \eta_l(E_F). \quad (16)$$

The location of the Fermi energy with respect to the muffin-tin potential is illustrated in figure 2. The multiple-scattering term  $N_m(E_F)$  has been neglected. This point may be a weakness of the approach since its importance has not been checked for computational reasons.

### 2.3. Our method

Presently we propose a new procedure based on the following arguments. The free boundary condition for the single-site scattering (equation (13)) is a good approximation only for a free conduction band whose energy starts at the muffin-tin zero [28, 29]. It appears that for liquid germanium the bottom of the conduction band calculated with Ziman's method [15], amounts

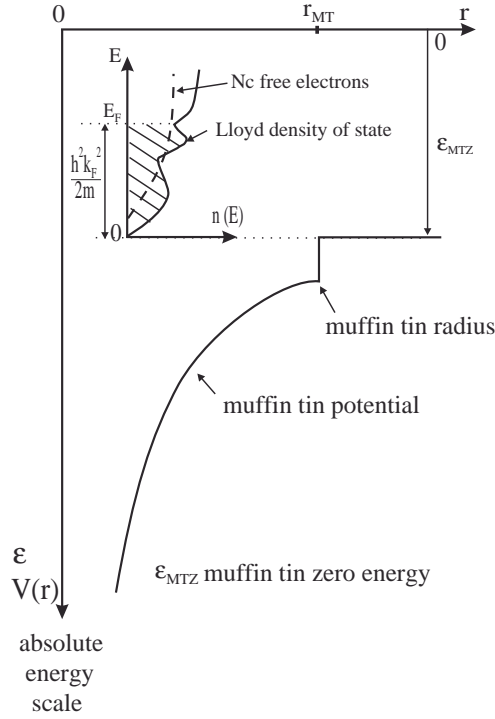


**Figure 2.** Determination of the Fermi energy following the method of Esposito *et al* [16].

−0.334 Ryd, showing a discrepancy with the free band approximation. We think that both Esposito's and Dreirach's approaches are not suited to obtain the correct germanium Fermi level. In Esposito's model the density of states is counted from the muffin-tin zero. However the bottom of the band as calculated from the Ziman formula is located far below it. The use of the free electron density in Dreirach's model is on one hand not close enough to the real density of states, and on the other hand, an important part of the band is situated below the muffin-tin potential. In order to improve the determination of the Fermi level we suggest introducing the free boundary conditions for the conduction bands of liquid germanium. This can be achieved by adjusting the bottom of the low-lying conduction band with the muffin-tin zero. We use a self-consistent procedure (figure 3) in which the muffin-tin zero is allowed to move downward (or upward) until the calculated bottom of the conduction band ( $E_B$ ) and the muffin-tin zero match within 0.001 Ryd. At each iteration equations (13) and (14) have to be satisfied. The muffin-tin zero together with the bottom of the conduction band are simultaneously displaced.

### 3. Resistivity and thermoelectric power

Ziman [22] proposed a formalism to interpret the electronic transport properties of normal metals. It has been adapted (in terms of phase shifts) to noble metals by Evans *et al* [30] and has been further extended to transition metals and alloys by Dreirach *et al* [9]. The electrical resistivity of a pure liquid metal can be written as a function of energy  $E$  and wave vector  $k$ :

$$\rho(E) = \frac{3\pi^2 m_e^2 \Omega_0}{4e^2 \hbar^3 k^6} \int_0^{2k} a(q) |t(q, E)|^2 q^3 dq \quad (17)$$





#### 4. Results and discussion

We employed the direct contact four-probe technique to perform the experimental resistivity and the small  $\Delta T$  method [32] to obtain the experimental thermopower. Our values for the resistivity (figure 4) and the thermopower (figure 5) are respectively  $67.98 \mu\Omega \text{ cm}$  and  $-0.23 \mu\text{V } ^\circ\text{C}^{-1}$  at  $950 \text{ } ^\circ\text{C}$ . The temperature dependence law is reported in both figures. These values are in good agreement with the results reported by Koubaa and Gasser [33] and more recently by Schnyders *et al* [34]. In order to reproduce the latter experimental electronic transport properties of liquid germanium, several prime calculations have been done, within the pseudopotential models. Koubaa and Gasser [33] and Schnyders *et al* [34] have used the Bachelet–Hamann–Schlüter [35] non-local pseudopotential. Their calculated values for the thermopower are relatively good but the resistivities are far below our experimental results. On the other hand, Waseda and Suzuki [36] have used the framework of the single site *t*-matrix approach together with the approach of Dreirach [8] for the determination of the Fermi energy and the one of Slater for the exchange potential. Their calculated results become fortuitously close to the experimental measurements. The recent experimental and calculated resistivity and thermopower values are summarized in table 1.

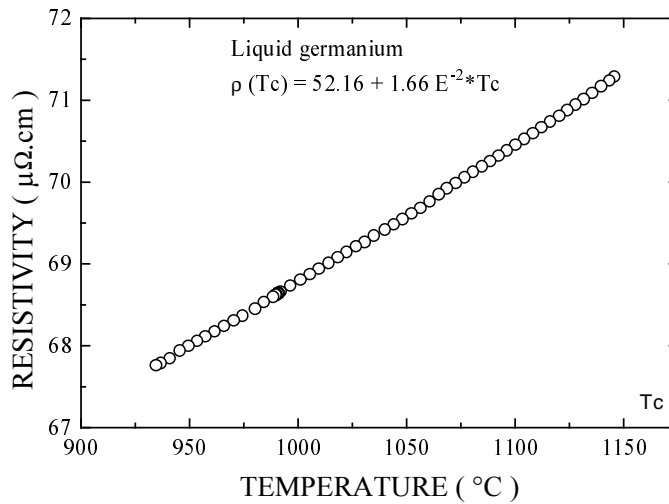


**Figure 4.** Experimental electrical resistivity of pure liquid germanium as a function of temperature.

**Table 1.** Comparison between recent experimental and calculated resistivities and thermopower values of liquid germanium.

	$\rho_{exp.} (\mu\Omega \text{ cm})$	$\rho_{calc.} (\mu\Omega \text{ cm})$	$Q_{exp.} (\mu\text{V } ^\circ\text{C}^{-1})$	$Q_{exp.} (\mu\text{V } ^\circ\text{C}^{-1})$
Schnyders and Van Zytveld [34]	66.8	41.2	-0.3	
Koubaa and Gassar [33]	67.8	55	-0.4	-2.2
Waseda and Suzuki [36]		66.2		-3.2
This work	$67.98 \pm 0.30$	see table 2	$-0.23 \pm 0.40$	see table 2

The present calculations were performed with the three kinds of muffin-tin potential recorded in section 1. The experimental radial distribution function and the corresponding structure factors used respectively in the superposition procedure and in the calculation of

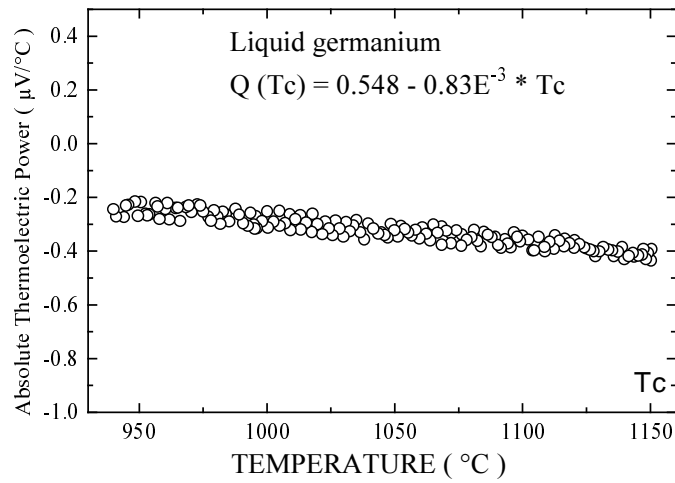


**Figure 5.** Experimental thermopower of pure liquid germanium as a function of temperature.

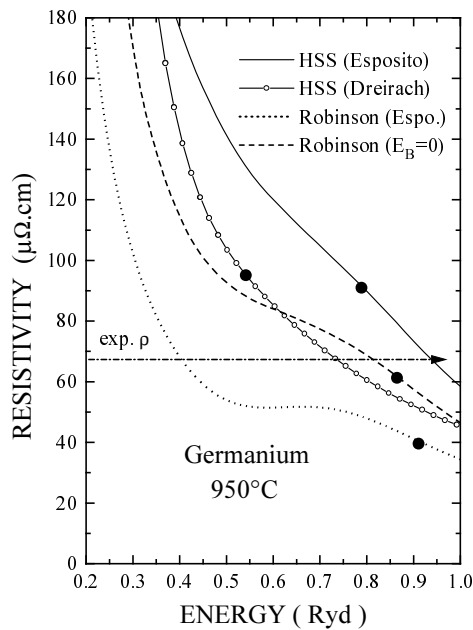


**Figure 6.** Energy dependence of the electrical resistivity of liquid germanium. Calculations were made using the neutral pseudoatom approach with Robinson's correction and are compared to the HSS approach and to our experimental data.

electronic transport properties have been measured by Bellissent-Funel and Bellissent [2, 26]. The resistivity and the thermopower are calculated as a function of energy from the muffin-tin zero potential to 1 Rydberg with the Herman–Skillman–Slater potential. The Ziman expression of the resistivity  $\rho(E)$  includes two parameters:  $k$  which appears in the prefactor and in the upper limit of the integral and  $E$  which appears in the expression of the  $t$ -matrix through the phase shifts which are a function of energy. In the Esposito approach ( $E_B = 0$ ) both

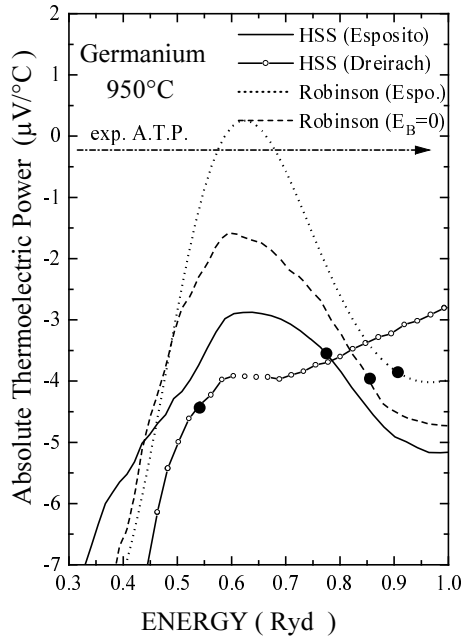


**Figure 7.** Energy dependence of the thermopower of liquid germanium. Calculations were made using the neutral pseudoatom approach with Robinson's correction and are compared to the HSS approach and to our experimental data.

parameters are bound by a relation  $E = \hbar^2 k^2 / 2m$  and are dependent. In our calculation  $k$  and  $E$  are correlated and varied simultaneously. We can consider that we increase the number of electrons  $N_C$ , that the Fermi sphere is expanded and that simultaneously the Fermi energy increases above the muffin-tin zero energy. This leads to a first resistivity and thermopower versus energy curve indicated 'HSS (Esposito)' in figures 6 and 7.

In the second approach we have a value of  $E_B$  different from zero. The resistivity is a function of  $k$ ,  $E$  and  $E_B$  and we have one relation between these parameters:  $E = E_B + \hbar^2 k^2 / 2m^*$ . So we have to deal with two independent parameters. The bottom of the energy band has been calculated following the Ziman formula [15]. We obtained  $-0.334$  Ryd for liquid germanium at  $950^\circ\text{C}$  (Dreirach obtained  $-0.31$  Ryd). The resistivity and thermopower curves are different for each  $E_B$ . The second curves obtained with that value of  $E_B$  are indicated 'HSS (Dreirach)' in figures 6 and 7.

We improved the electron correlation contribution using the expression of Robinson *et al* [18] for the average screened exchange potential expressed in formula (3). We obtain a third resistivity and thermopower versus energy curve in figure 6 and 7 denoted 'Robinson (Esposito)' to indicate that we used the Robinson contribution with Esposito's approach ( $E_B = 0$  and the density of state obtained with the Lloyd formula). With this correction we obtained a lower resistivity versus energy curve which indicates a very important modification of the electronic transport properties if the exchange contribution is properly taken into account. However this approach is not even fully consistent. It remains that the Ziman formula gives an  $E_B$  value which is non-negligible. Thus we achieve the consistency of the calculation by our approach presented in section 2.3. We obtained the curve indicated 'Robinson ( $E_B = 0$ )' corresponding to the HSS potential with Esposito's approach for the Lloyd density of states, with Robinson's correction and with the self-consistent determination of the muffin-tin zero

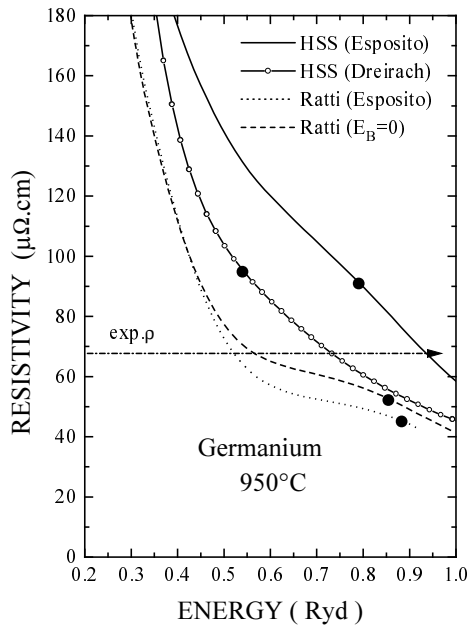


**Figure 8.** Energy dependence of the electrical resistivity of liquid germanium. Calculations were made with the Ratti ionic approach and are compared to the HSS approach and to our experimental data.

potential. The curve is increased from 20 to 40  $\mu\Omega$  cm compared to the third curve (Robinson (Esposito)) and is near the second curve (HSS (Dreirach)). To compare with the experimental resistivity and thermopower it is necessary to determine the Fermi energy by filling the density of states curve with the four valence electrons of germanium. The Fermi energies are very different for the different curves. They are indicated by dots on the resistivity and thermopower versus energy curves and their numerical values are reported in table 2. In this table we give two values for the thermopower. The first value corresponds to the local approximation ( $\chi = 3 - 2\alpha$ ). The second value is the full energy dependent expression ( $\chi = 3 - 2\alpha - \beta/2$ ).

#### 4.1. HSS and Robinson's correction

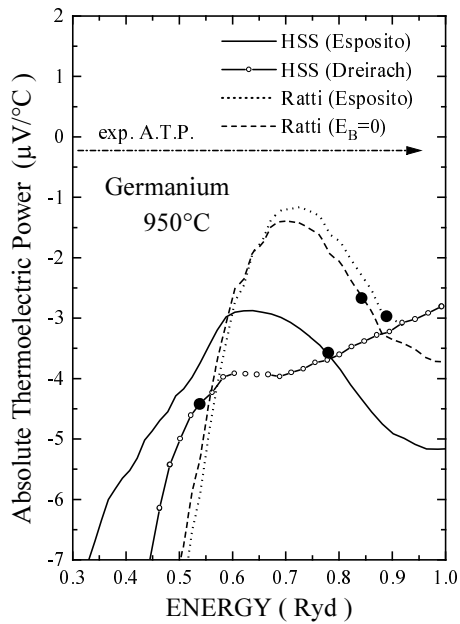
We observe that the HSS potential combined with the Fermi energy determination given by Dreirach and Esposito leads to resistivity values (96 and 92  $\mu\Omega$  cm respectively) larger than the experimental value (68  $\mu\Omega$  cm). The resistivity obtained with Robinson's potential in which the effects of the electron correlation are taken into account are below the values found with the HSS potential. It stresses the particular importance of the Fermi energy determination. It is clear that the best result is obtained with the fourth curve (Robinson ( $E_B = 0$ )) where we obtain a resistivity of 62  $\mu\Omega$  cm compared to the experimental one of 68  $\mu\Omega$  cm. Considering the thermopower, all the calculations give results between  $-3.5$  and  $-4.5$   $\mu\text{V}^\circ\text{C}^{-1}$  which indicate that the thermopower is not sensitive to the method of calculation. All calculated resistivities and thermopower for various muffin-tin potentials are reported in table 2.

#### 4.2. Ionic potential

The resistivity and thermopower calculated with Ratti's potential, supplemented by the Ichimaru-Utsumi [38] dielectric screening function, are presented in figures 8 and 9 together with the curves previously calculated with the HSS potential. The closest value to the experimental resistivity is again that obtained with our self-consistent calculation and Fermi

**Table 2.** Fermi energy ( $E_F$ ), effective number of conduction electrons ( $N_C$ ), resistivity ( $\rho(E_F)$ ) and thermopower ( $Q(E_F)$ ) of liquid germanium.

	$E_F$ (Ryd)	$N_C$	$\rho(E_F)$ ( $\mu\Omega$ cm)	$Q(E_F)$ ( $\mu\text{V } ^\circ\text{C}^{-1}$ ) local approximation	$Q(E_F)$ ( $\mu\text{V } ^\circ\text{C}^{-1}$ ) full calculation
HSS (Dreirach)					
$E_B = -0.334$ (Ryd), $m^* = m_e$	0.535	4	96.12	-0.91	-4.45
HSS (Esposito)	0.787	3.452	91.92	+5.13	-3.76
Robinson (Esposito)	0.913	4.381	40.51	+5.27	-3.87
Robinson ( $E_B = 0$ )	0.861	3.942	61.96	+6.11	-4.11
Ratti (Esposito)	0.884	4.038	45.26	+4.69	-2.94
Ratti ( $E_B = 0$ )	0.846	3.846	52.89	+5.41	-2.70
LDA (Esposito)	0.886	4.075	53.45	+5.05	-1.79
LDA ( $E_B = 0$ )	0.851	3.875	62.90	+5.19	-1.75
GGA (Esposito)	0.891	4.152	46.57	+4.82	-1.63
GGA ( $E_B = 0$ )	0.868	3.987	55.96	+5.43	-1.78
Exp. (present work and [37])			67.98	-0.23	-0.23

**Figure 9.** Energy dependence of the thermopower of liquid germanium. Calculations were made with the Ratti ionic approach and are compared to the HSS approach and to our experimental data.

energy determination. The thermopower values calculated with Ratti's potential shift slightly towards the experimental value as can be seen on figure 9.

#### 4.3. Density functional theory

Within the free boundary condition the calculated resistivities and thermopowers obtained in the simple LDA and the generalized gradient approximation are presented in figures 10 and 11. The GGA proposed by Perdew and Wang [20] has also been used. It appears that

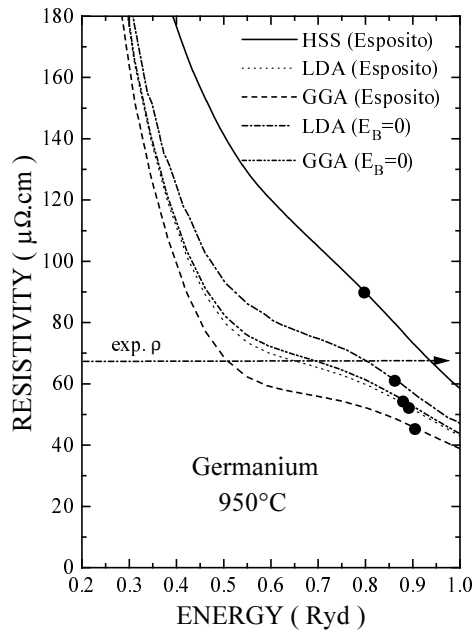


**Figure 10.** Energy dependence of the electrical resistivity of liquid germanium. Calculations were made using the neutral pseudoatom approach with LDA and GGA and are compared to the HSS approach and to our experimental data.

the LDA results are very close to the measured resistivity value, even better than the GGA result. The density functional theory improves the HSS approach for the obvious reason that it includes a correlation term. The GGA introduced to take care of the inhomogeneity [39] of the electron density does not confirm an expected better result. The calculated thermopower values are very closer the experimental value than those obtained with the previous approaches:  $-1.75 \mu\text{V}^\circ\text{C}^{-1}$  and  $-1.78 \mu\text{V}^\circ\text{C}^{-1}$  respectively for LDA and GGA compared to an experimental value of about  $-0.23 \mu\text{V}^\circ\text{C}^{-1}$ .

In order to verify the free boundary conditions, Esposito *et al* [16] introduced the so-called effective valence  $N_C$  in place of the pure valence  $Z$ , as such an  $N_C$  can be interpreted as giving the same free electron density of states as the real one. Within that description each germanium atom loses its four valence electrons to form the conduction band. It implies that if the density of states is free electron like,  $N_C$  should display a value close to four electrons. Considering the results of table 2,  $N_C$  is very near the value of four for all the potentials including a correlation contribution (Robinson, Ratti, LDA). The sole exception concerns the HSS potential where only the exchange term is taken into account.

We can also deduce from the results of table 2 that the determination of the Fermi level with Esposito's procedure and the subsequent resistivity derivation leads to underestimated values for the resistivity (except the HSS potential). As the resistivity decreases when the charge carrier concentration increases, the theoretical results should be improved either if  $N_C$  decreases or if the  $\rho(E)$  curve is shifted to higher values. The application of the free boundary conditions to the liquid conduction band suggested in the present work achieves these two goals. The inspection of table 2 and figures 6, 8 and 10 shows that our correction raises the resistivity. For each potential, the two quantities evolve in the right way and provide a justification of the use our self-consistent method. We can also observe in table 2 the very

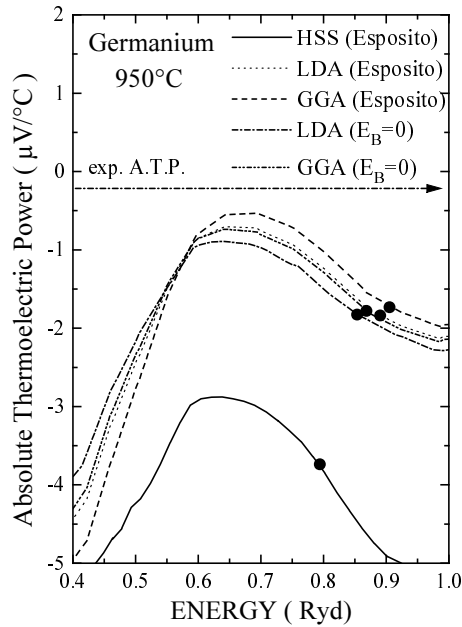


**Figure 11.** Energy dependence of the thermopower of liquid germanium. Calculations were made using the neutral pseudoatom approach with LDA and GGA and are compared to the HSS approach and to our experimental data.

important contribution of the  $t$ -matrix energy dependence that corrects the local approximation from 3.5 to 10.2  $\mu\text{V K}^{-1}$ . It is evident that the energy dependent contribution plays a very important role and cannot be neglected.

## 5. Conclusion

We would like to emphasize that there was an uncertainty in the determination of the Fermi level since the construction of the muffin-tin potential and the derivation of the one electron energy spectrum are treated separately. Indeed, the *ab initio* self-consistent methods intensively developed for ordered solids to obtain the electronic ground state were largely missing for not well organized materials. The electronic density of states and the muffin-tin potential for liquids metals were not self-consistently positioned with respect to each other. This puzzling point received two different answers within the works of Dreirach [8] and Esposito *et al* [16]. To cope with the difficulty both authors proposed a different prescription for the Fermi energy determination. In this paper a combination of the two prescriptions has been presented added to a consistent determination of the Fermi energy when free boundary conditions are considered.

We compared three different points of view (Hartree–Fock and neutral pseudoatom, Hartree–Fock and ionic plus electronic potentials and finally DFT). We first included the correlation contribution in two first schemes (which reduced drastically the resistivity) and compared to the LDA result. All these values are too low. Then we correct the three results by matching self-consistently the bottom of the band with the muffin-tin zero potential. The calculated resistivities are considerably improved, the LDA method giving a result (62.9  $\mu\Omega\text{ cm}$ ) approximately the same as the Robinson method (62.0  $\mu\Omega\text{ cm}$ ) to be compared to the experimental one (67.8  $\mu\Omega\text{ cm}$ ). For the various approaches based on muffin-tin potentials including the correlation effect, the free boundary condition improves always the quality of the



results. The LDA method gives better results for the thermopower ( $-1.75 \mu\text{V}^\circ\text{C}^{-1}$ ) than the Robinson method ( $-4.11 \mu\text{V}^\circ\text{C}^{-1}$ ) compared to our experimental value of  $-0.23 \mu\text{V}^\circ\text{C}^{-1}$ . This study allows us to stress two observations: first the calculated results are very sensitive to the potential used, second the density functional theory with the standard LDA approximation gives the best results both for the resistivity and the thermopower. This observation is not surprising since the LDA is now widely used in solid electronic structure calculation owing to its success over other approaches.

## References

- [1] Petkov V, Takeda S, Waseda Y and Sugiyama K 1994 *J. Non-Cryst. Solids* **168** 97
- [2] Bellissent M C and Bellissent R 1984 *J. Non-Cryst. Solids* **65** 383
- [3] Indlekofer G, Oelhafen P, Lapka R and Güntherodt H J 1988 *Z. Phys. Chem.* **157** 465
- [4] Jank W and Hafner J 1990 *Phys. Rev. B* **41** 1497
- [5] Ziman J M 1964 *Adv. Phys.* **13** 89
- [6] Slater J C 1951 *Phys. Rev.* **81** 385
- [7] Kohn W and Sham L 1965 *Phys. Rev. A* **140** 1133
- [8] Dreirach O 1971 *J. Phys. F: Met. Phys.* **1** L40
- [9] Dreirach O, Evans R, Güntherodt H J and Künzi U 1972 *J. Phys. F: Met. Phys.* **2** 709
- [10] Hirata K, Waseda Y, Jain A and Srivastava R 1977 *J. Phys. F: Met. Phys.* **7** 419
- [11] Ratti V K and Jain A 1973 *J. Phys. F: Met. Phys.* **3** L69–74
- [12] Ratti V K 1972 *Thesis* University of Bristol
- [13] Mukhopadhyay G, Jain A and Ratti V K 1973 *Solid State Commun.* **13** 1623
- [14] Waseda Y 1980 *The Structure of Non-crystalline Materials* (New York: McGraw-Hill)
- [15] Ziman J M 1967 *Phil. Mag.* **6** 701
- [16] Esposito E, Ehrenreich H and Gelatt C D 1978 *Phys. Rev. B* **18** 3913
- [17] Lloyd P 1967 *Proc. Phys. Soc.* **90** 207
- [18] Robinson J E, Bassani F, Knox R S and Shrieffer J R 1962 *Phys. Rev. Lett.* **9** 215
- [19] Von Barth U and Hedin L 1972 *J. Phys. C: Solid State Phys.* **5** 1629
- [20] Perdew J P and Wang Y 1986 *Phys. Rev. B* **33** 8800
- [21] Perdew J P 1986 *Phys. Rev. B* **33** 8822
- [22] Ziman J M 1961 *Phil. Mag.* **6** 1013
- [23] Herman F C and Skillman S 1963 *Atomic Structure Calculation* (Englewood Cliffs, NJ: Prentice-Hall)
- [24] Slater J C 1951 *Phys. Rev.* **82** 538
- [25] Hohenberg P and Kohn W 1964 *Phys. Rev. B* **136** 864
- [26] Mattheiss L F 1964 *Phys. Rev. A* **133** 1399
- [27] Bellissent-Funel M C and Bellissent R 1980 Réunion des liquides et amorphes métalliques, Grenoble and private communication
- [28] Faber T E and Ziman J M 1965 *Phil. Mag.* **11** 153
- [29] Delley B, Beck H, Künzi H-U and Güntherodt H-J 1978 *Phys. Rev. Lett.* **40** 193
- [30] Delley B and Beck H 1979 *J. Phys. F: Met. Phys.* **9** 517
- [31] Evans R, Greenwood D A and Lloyd P 1971 *Phys. Lett. A* **35** 57
- [32] Vinckel J, Hugel J and Gasser J-G 1996 *Phil. Mag. B* **73** 231
- [33] Vinckel J 1994 *Thèse* Université de Metz
- [34] Koubaa N and Gasser J G 1990 *J. Phys.: Condens. Matter* **2** 2297
- [35] Schnyders H S and Van Zytveld J B 1996 *J. Phys.: Condens. Matter* **8** 10 875
- [36] Bachelet G B, Hamann D R and Schlüter M 1982 *Phys. Rev. B* **26** 4199
- [37] Waseda Y and Suzuki K 1975 *Z. Phys. B* **20** 339
- [38] Makradi A 1997 *Thèse* Université de Metz
- [39] Ichimaru S and Utsumi K 1981 *Phys. Rev. B* **24** 7385
- [40] Moll N, Bockstedte M, Fuchs M, Pehlke E and Scheffler M 1995 *Phys. Rev. B* **52** 2550